

# A heat transfer model for slug flow in a horizontal tube

G. Sun<sup>a</sup>, G.F. Hewitt<sup>a,\*</sup>, V.V. Wadekar<sup>b</sup>

<sup>a</sup> Department of Chemical Engineering, Chemical Technology and Medicine, Imperial College of Science, Prince Consort Road, London SW7 2BY, UK

<sup>b</sup> HTFS, Aspen Technology, Harwell, Oxfordshire OX1 0QR, UK

Received 22 August 2001; received in revised form 15 October 2003

## Abstract

A new model is presented for the analysis of hydrodynamics and heat transfer which can be used to predict heat transfer coefficients in horizontal slug flow.

The results of Jung [Horizontal-flow boiling heat transfer using refrigerant mixtures, EPRI Rep., 1989, ER-6364] show a considerable variation of the heat transfer coefficient around the periphery of the tube at low qualities, with the top of the tube having the highest coefficient. It is shown that this region is likely to be one in which slug flow occurs. The transition into the low quality regime is shown to be closely associated with that into slug flow, using an existing flow pattern map.

The model follows the traditional interpretation of evaporative heat transfer, namely that of forced convective heat transfer which may be enhanced by bubble nucleation processes. Slug flow hydrodynamic parameters such as liquid slug and inter-slug (“film”) lengths to total slug unit length, and the top and bottom film thickness and liquid film velocities in the inter-slug regions are important in understanding the heat transfer phenomena. Therefore, heat transfer models developed for pipe top and bottom should include the effects of these slug flow parameters.

© 2003 Elsevier Ltd. All rights reserved.

## 1. Introduction

Heat transfer during two-phase vapour–liquid flow is widely encountered in industrial operation. It occurs during vaporisation and condensation processes such as in boilers, condensers and many other major items of chemical and power plants and water-cooled nuclear reactors is dependent upon a knowledge of the fluid dynamics and heat transfer process occurring during forced convective boiling and condensation. However, in spite of the very large amount of work which has been done in this field, the state of knowledge is such that reliable design methods are not available for two-phase flow due to its very complex nature.

Slug flow that can exist over a wide range of phase velocities is characterised by the alternative passage of

liquid slugs and gas bubbles. The liquid slug that may be aerated at high gas velocities is considered to fill the entire cross section of the pipe, whereas a gas slug occupies only a fraction of the cross section. Because of the effect of gravity, gas slugs are concentrated in the upper of the pipe in horizontal flow. Thus, gas and liquid slugs are alternatively in contact with the pipe top, and a continuous liquid phase is in contact with the pipe bottom. The liquid slug picks up liquid at the slug nose and sheds back the liquid in the form of slow-moving film. For viscous liquids or small tube diameters, there might be a thin, relatively stationary liquid film at the pipe top. Thus, the unsteady nature of slug flow may cause substantial variations in wall temperatures and in peripheral heat transfer rates, especially when a constant heat flux condition is employed.

Jung [1] studied the evaporation of refrigerant-12 in a 9 mm tube and made measurements of the heat transfer coefficient at the top of the tube, at the bottom of the tube and in a position halfway around the periphery between the two (designated “middle” in what follows).

\* Corresponding author. Tel.: +44-171-594-5562; fax: +44-171-594-5564.

E-mail address: [g.hewitt@ic.ac.uk](mailto:g.hewitt@ic.ac.uk) (G.F. Hewitt).

The results are exemplified in Fig. 1. At high qualities, there is some variation around the tube periphery, with the heat transfer coefficient at the top being somewhat higher than the heat transfer coefficient at the bottom. This is typical of annular flow where the heat transfer is likely to be mainly controlled by forced convective mechanisms (i.e. with nucleation largely suppressed). At low qualities however, there are gross differences between the top and bottom of the tube as shown and it seems likely that this can be ascribed to a change in the flow regime.

Non-evaporative heat transfer in air–water flow in tubes has been studied by Shoham et al. [2], Kago et al. [3] and Deshpande et al. [4]. The kind of result obtained is typified by those shown in Fig. 2. In these air–water

flow situations, the coefficient at the top of the tube is much lower than the coefficient at the bottom. Thus, the situation is quite different from that seen in evaporation as shown in Fig. 1.

This interesting difference between the two results can be ascribed to a number of factors as follows:

- (1) In the air–water experiments, the liquid film at the top of the channel could be drying out, with a consequent drastic reduction of the heat transfer coefficient in that region.
- (2) There is an important difference between evaporative and non-evaporative heat transfer. In evaporative heat transfer, the interface temperature is constant at the saturation temperature. In non-evap-

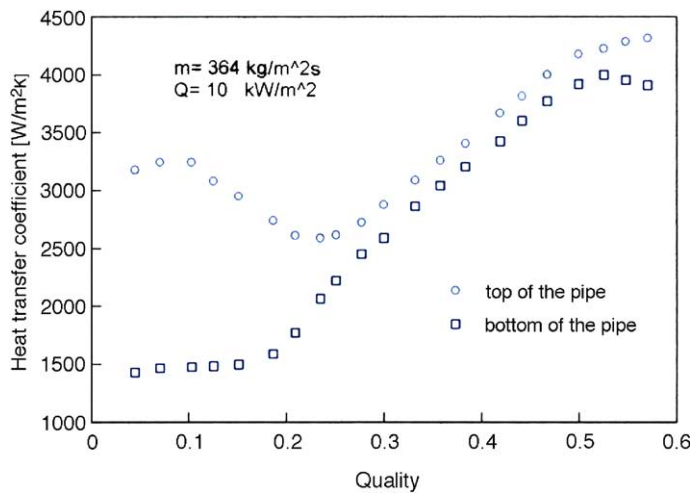


Fig. 1. Experimental data of Jung [1].

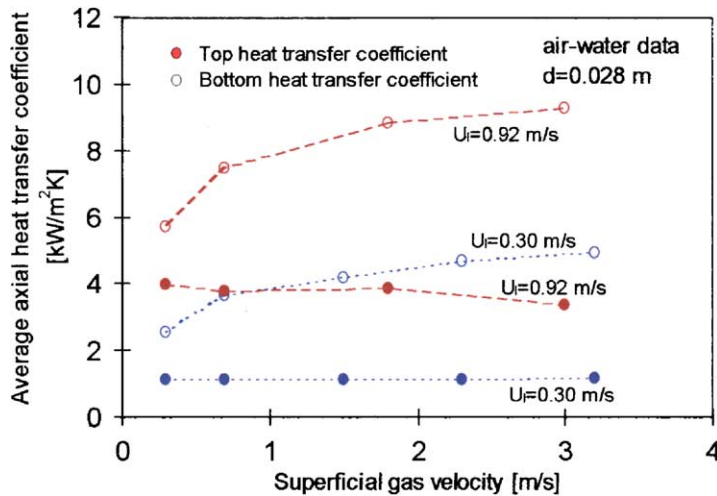


Fig. 2. Data of Deshpande et al. [4].

orative heat transfer, the interface temperature may change with distance and with peripheral position. Supposing we had a system with a constant wall temperature; if there is restricted mixing around the periphery of the tube in the film region of a slug flow or, alternatively, in an annular flow, then the thin liquid layer at the top would approach the wall temperature and would reduce the amount of heat transfer. The thick layer of liquid at the bottom of the tube, on the other hand, would take much longer to approach the wall temperature and would therefore appear to have a very higher heat transfer coefficient. In other words, what might be seen in this case is a non-uniform liquid temperature rather than a maldistribution of the heat transfer coefficient. Though Deshpande et al. used electrical heating, it is noted that the tube wall thickness that they employed was quite large and circumferential conduction may have tended to make their experiments more representative of a constant wall temperature rather than constant wall heat flux. There is some further evidence of restricted circumferential mixing in two-phase annular and slug flow from the work of Jung et al. [1] on multicomponent evaporation. In this case, the less volatile component tends to become more concentrated at the top of the tube and this gives an *apparent maldistribution* of heat transfer coefficient (based on the mixture properties). In the experiments of Jung et al. [1] the heat transfer coefficient at the top of the tube was apparently lower than that at the bottom for some situation even in the case of evaporation.

- (3) The experiments of Deshpande et al. [4] were conducted in a much larger (28 and 57 mm) tubes and this would give a larger propensity for dryout than the small diameter tube used by Jung [1].

The objective of the present work was to provide a rational framework for the interpretation of the results of Jung [1]. The questions addressed were as follows:

- (1) Is the observed transition between the low quality and high quality regimes (see Fig. 1) consistent with the predictions from established flow pattern transition maps (such as the map of Taitel and Dukler [5])?
- (2) Within the slug flow regime itself, what are the predicted slug lengths, film thickness etc.?
- (3) What are the mechanisms governing heat transfer in the respective regions of the slug flow?
- (4) Can quantitative predictions of the heat transfer coefficients be made?

In what follows below, the flow regime transition will be discussed in Section 2. This is followed by a description how to obtain hydrodynamic parameters in

slug flow in Section 3. A study of liquid behaviour in the film region will be presented in Section 4. A new correlation for heat transfer coefficient in horizontal slug flow will be described in Section 5. Finally, concluding remarks will be given in Section 6.

## 2. Flow regime transition

One of the most widely used flow pattern transition maps is that due to Taitel and Dukler [5] and this map has been selected for comparison with the Jung data [1]. It is recognised that some deficiencies in the Taitel and Dukler map have emerged in subsequent work, notably in its failure to take adequate account of physical property variations (see for instance Weisman et al. [15]). However, the Weisman et al. work suggests that the effects of surface tension and gas density may be counteracting in the case of refrigerant/refrigerant vapour mixtures and that the deficiencies in the Taitel–Dukler map may be less serious in this case.

The Taitel and Dukler [5] map is semi-theoretical in nature and plots the transition in terms of the number of dimensionless groups. Here, we are concerned primarily with the slug flow to annular flow transition. In this map, it is suggested that when the equilibrium liquid level in the pipe is above the pipe centre line, intermittent flow will develop, and if  $h_L/D < 0.5$  (where,  $h_L$  is the liquid level), annular or annular dispersed liquid flow will result. Since transition takes place at a constant value of  $h_L/D = 0.5$ , The Taitel–Dukler [5] analysis indicates that a single value of the Martinelli parameter  $X_{tt}$  characterises the change in regime. The Martinelli parameter is defined as

$$X_{tt} = \left[ \frac{(dp_F/dz)_L}{(dp_F/dz)_G} \right]^{\frac{1}{2}} \quad (1)$$

where  $(dp_F/dz)_L$  and  $(dp_F/dz)_G$  are the pressure gradients for the flow of liquid and gas phases flowing alone in the channel respectively.

For a horizontal tube, the transition value is  $X_{tt} = 1.6$ , and this is plotted in Fig. 3 as boundary B. A further boundary in the Taitel–Dukler flow pattern map is the limit of the stratified regime A–A which is plotted in terms of the parameter  $F$  (the Froude number modified by the density ratio) and the Martinelli parameter respectively as shown in Fig. 3.  $F$  is defined as follows:

$$F = \sqrt{\frac{\rho_G}{(\rho_L - \rho_G)}} \frac{U_G}{\sqrt{Dg}} \quad (2)$$

where  $\rho_G$  and  $\rho_L$  are the densities of the gas and liquid phase respectively,  $U_G$  is the superficial gas velocity,  $D$  the tube diameter,  $g$  the acceleration due to gravity. As will be seen in Figs. 3–5, for  $X_{tt} < 1.6$ , the transition of stratified flow is into annular flow whereas for  $X_{tt} > 1.6$ , the transition is into slug flow.

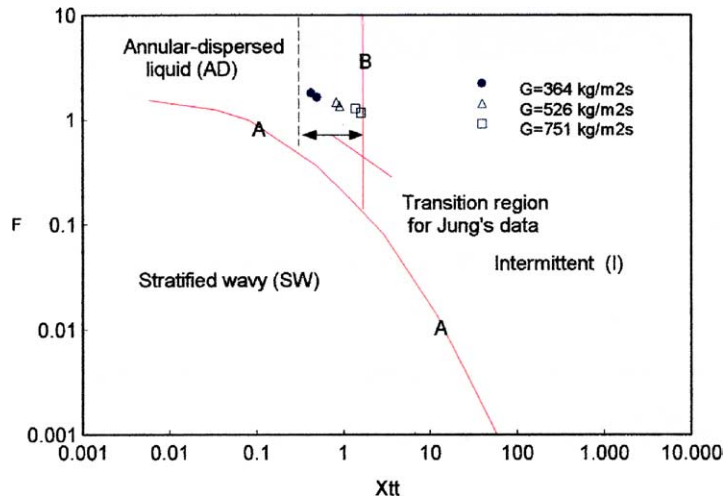


Fig. 3. Flow pattern transition map of Taitel and Dukler [5].

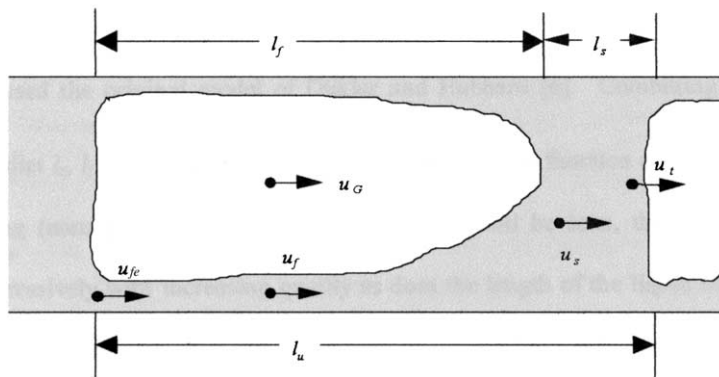


Fig. 4. The physical model for slug flow.

The transition between the lower quality (large radial variation) region and the high quality (smaller radial variation) region as shown in Fig. 1 can be plotted in terms of the above parameters. Of course, one can only specify a *range* of qualities over which the transition occurred.

For the experiments of Jung [1] the following approximate quality ranges for the transition were estimated:

0.22–0.25 for a mass flux of 364 kg/m<sup>2</sup>s

0.13–0.14 for a mass flux of 526 kg/m<sup>2</sup>s

0.07–0.08 for a mass flux of 751 kg/m<sup>2</sup>s

These ranges are plotted on Fig. 3 and it will be seen that, indeed, the transition ranges are quite close to the predicted slug flow boundary and lie in the range  $0.65 < X_{tt} < 1.6$  (the lower boundary of this range is

shown as the dotted line in Fig. 3). This corresponds to a range of  $h_L/D$  of 0.35–0.5. In fact, the accuracy of the Taitel–Dukler slug–annular transition prediction is not very high, with considerable variations observed in the literature (see for instance Reimann et al. [14]).

We conclude that it can be reasonably adduced (subject to the uncertainties found in all flow pattern predictions) that the observed transition in Fig. 1, is indeed, a transition from annular to slug flow.

### 3. Hydrodynamic parameters in slug flow

To calculate the characteristics of the slug flow, we use the well-established model of Dukler and Hubbard [6] with some modifications to take account of recent work. Dukler and Hubbard [6] define a *slug unit* which consists of the liquid slug (where the liquid phase is

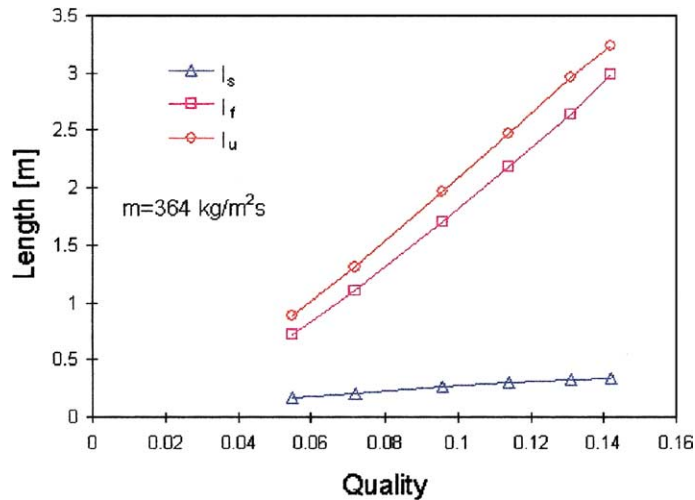


Fig. 5. Lengths of the slug, film and slug unit.

continuous and occupies the whole cross section of the pipe) and a *film region*, namely the region between the slugs (see Fig. 4). The length of the liquid slug and film regions are defined as  $l_s$  and  $l_f$  and Dukler and Hubbard [6] defined a total slug unit as given by

$$l = l_s + l_f = \frac{(1 + C)U}{v_s} \quad (3)$$

where  $v_s$  is the slug frequency,  $U$  the total superficial velocity, and  $C$  a parameter which has the value of the order of 0.25, which is related to the shedding rate of liquid by the slug into the film region.

The slug length is given by the equation:

$$l_s = \frac{U}{v_s(\varepsilon_{Ls} - \varepsilon_{Lf})} \left[ \frac{U_L}{U} - \varepsilon_{Lf} + C(\varepsilon_{Ls} - \varepsilon_{Lf}) \right] \quad (4)$$

where  $U_L$  is the liquid superficial velocity,  $\varepsilon_{Ls}$  and  $\varepsilon_{Lf}$  are the liquid hold-up (fraction of the cross section occupied by the liquid) in the slug region and the film region respectively, and  $U$  is the total superficial velocity. Here, we have used the correlation of Heywood and Richardson [7] for  $v_s$  and for the hold-up in the slug ( $\varepsilon_{Ls}$ ) we have used the correlation of Gregory and Scott [8].

$$v_s = 0.0364 \left[ \frac{U_L}{U} \left( \frac{2.02}{D} + \frac{U^2}{gD} \right) \right]^{1.08} \quad (5)$$

$$\varepsilon_{Ls} = \left[ 1 + \left( \frac{U_L}{8.66} \right)^{1.39} \right]^{-1} \quad (6)$$

where  $D$  is tube diameter.

For  $\varepsilon_{Lf}$ , we used the original model of Dukler and Hubbard [6]. Combining these models, it is possible to predict  $l_s$ ,  $l_f$  and  $l_u$ . These parameters are plotted as a function of quality for one mass flux studied by Jung

(namely  $364 \text{ kg/m}^2 \text{ s}$ ) in Fig. 5. As will be seen, the length of the slug unit increases progressively with increasing quality as does the length of the liquid slug. The liquid film region increases however much more rapidly, as shown. These data will be used in the ensuing analysis.

#### 4. Liquid behaviour in the film region

Once the slug has passed, a layer of liquid is left around the periphery of the tube, and the upper part of this layer begins to drain downwards, thinning the film at the top of the tube. This situation has been investigated in some detail by Coney [9] and this picture of what is happening is shown in Fig. 6. The situation being considered here is somewhat different since it is likely that the slugs with which we are dealing in the present paper would be more truly in the slug form rather than in the “frothy surge” form designated by Coney [9]. However, the analysis is still applicable since we are concerned mainly with prediction of what happens at the top of the tube and the picture will be similar. Thus, in the slug body, a boundary layer is built up terminating at the end of the slug. This boundary layer represents the starting point for the subsequent development of the film region. The variation of the thickness of the film at the top of the tube after this point is determined by the change in the velocity profile, by viscous draining and by evaporation of the liquid from the film.

The Coney analysis proceeds as follows:

- (1) The boundary layer thickness at the end of the slug region is predicted. This depends on the fluid physical properties and the velocity and length of the slug.

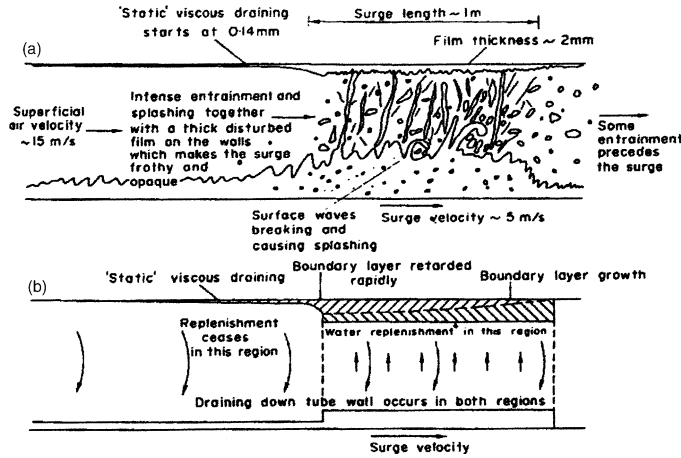


Fig. 6. Pictorial representation of replenishment and draining processes (not to scale). (a) The situation as it is in practice with some typical dimensions and velocity. (b) The idealised picture by Coney [9].

- (2) At the end of the slug, the outer edge of the boundary layer is moving at the slug velocity and this boundary condition is applied and the development of the liquid film determined, taking into account the draining and changes of the velocity profile. Evaporation is also considered.
- (3) Coney [9] was specifically interested in the point at which the film on the upper surface of the tube dried out. This could be determined by taking into account evaporation of the film since the drainage effect per se, although leading to vanishing the small films, it would not actually cause the film to dry out.

We have repeated in detail the Coney analysis for the present case. The variation of the thickness of the film as a function of the distance upstream from the edge of the slug has been calculated for the top of the channel. In no case in the analysis of the present data (where the heat flux effect was taken into account) did the upper film dry out. In analysing the heat transfer data, we are primarily concerned with averaging and the average film thickness  $\delta$  at the top of the tube was determined for each condition and the results obtained for this average are shown in Fig. 7. Further details of the calculation are given by Sun [16].

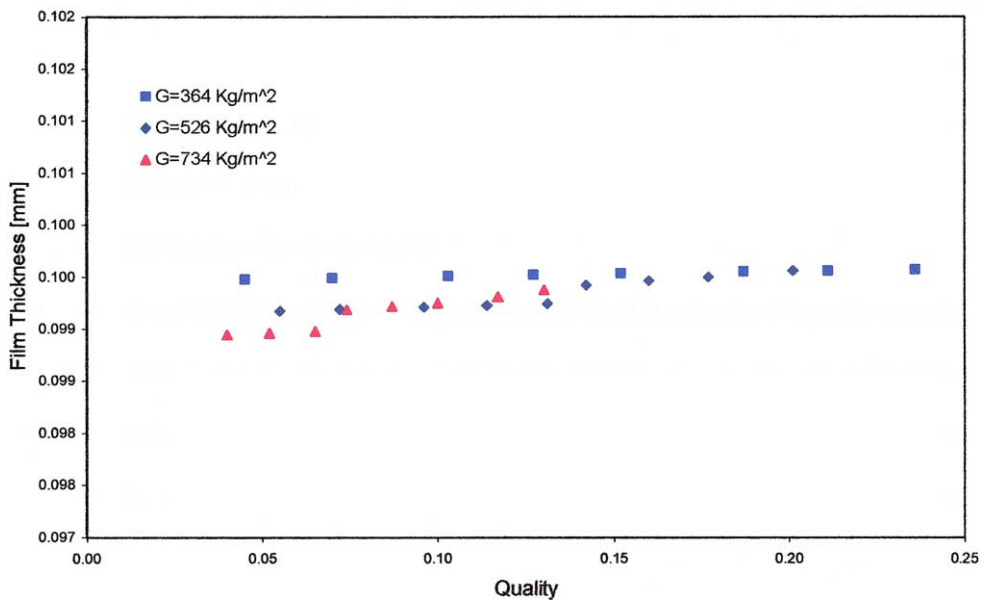


Fig. 7. Average film thickness at the top of the tube in the film region predicted by the analysis of Coney [9].

The average film thickness at the top of the tube was found to be around 0.1 mm and did not vary greatly from this value for the range of flow conditions investigated. The relative constancy of this film thickness is interesting, and perhaps surprising, but is consistent with the assumptions of the Coney analysis. The average values of film thickness and film velocity calculated in this exercise were used in the heat transfer calculations and correlations as described below.

## 5. Correlation of heat transfer coefficients

At the beginning of the present study, it was thought that the thinning of the liquid film at the top of the tube would actually give rise to a very high *convective coefficient* and that this would be the explanation of the gross variation of heat transfer coefficient with circumferential position in the slug flow regime. However, the results of the calculations using the Coney [9] analysis demonstrated that this initial explanation of the phenomenon was not correct. In fact, the calculations described show that the film at the top of the tube is moving less rapidly than that at the bottom and the suppression of nucleate boiling is less. Thus, surprisingly, nucleate boiling dominates the heat transfer at the top of the tube and forced convective at the bottom.

In the analysis reported here, the nucleate boiling coefficient is calculated from the correlation of Cooper [10] for both slug and film regions. For the forced convection coefficient in the film region we adapt the film heat transfer theory as reported by Hewitt and Hall-Taylor [11]. This correlation was developed for annular flow. Here, we use the same format but we employ the *calculated mean film thickness* and the *average velocity* at the top of the tube (estimated from the Coney, 1974 analysis) and the *calculated average thickness of the liquid layer* and *velocity* at the bottom of the tube (estimated from the analysis of Dukler and Hubbard [6]), both for the film region. For the forced convection coefficient in the slug region we adapt the correlation of Dittus–Boelter. The Cooper [10] correlation for nucleate boiling is as follows:

$$\alpha_{nb} = 55P_r^{0.12}(-\log_{10}P_r)^{-0.55}M^{-0.5}q^{0.67}S \quad (7)$$

where  $P_r$  is the reduced pressure,  $M$  molecular weight,  $q$  the heat flux. The suppression factor  $S$  accounts for the reduction of the nucleate boiling coefficient because of the flow is calculated from the relationship of Gungor and Winterton [12]:

$$S = \frac{1}{1 + 1.15 \times 10^{-6}E^2Re_L^{1.17}} \quad (8)$$

where

$$E = 1 + 24000Bo^{1.16} + 1.37(1/X_n)^{0.86} \quad (9)$$

where  $Bo$  is the boiling number ( $\dot{q}/h_{lg}G$ ), where  $h_{lg}$  is latent heat of evaporation and  $G$  is mass flux.

For the forced convective coefficient in the film region, we used the film heat transfer theory as reported by Hewitt and Hall-Taylor [11] and Hewitt et al. [13]. Thus

$$\alpha_{fc,f} = \frac{C_{pL}(\rho_L\tau_0)^{0.5}}{T^+} \quad (10)$$

where,  $\delta$  is the film thickness,  $\tau_0$  is interfacial shear stress:

$$\tau_0 = \frac{1}{\rho_L} \left( \frac{\delta^+ \rho_L \eta_L}{\delta} \right)^2 \quad (11)$$

$$\begin{aligned} T^+ &= \delta^+ Pr_L \quad \text{for } \delta^+ \leq 5 \\ &= 5 \{ Pr_L + \ln [1 + Pr_L(\delta^+/5 - 1)] \} \quad \text{for } 5 \leq \delta^+ \leq 30 \\ &= 5 \left\{ Pr_L + \ln [1 + 5Pr_L] + \frac{1}{2} \ln \frac{\delta^+}{30} \right\} \quad \text{for } \delta^+ > 30 \end{aligned} \quad (12)$$

$$\begin{aligned} \delta^+ &= 0.7071Re_f^{0.5} \quad \text{for } Re_f \leq 50 \\ &= 0.6323Re_f^{0.5286} \quad \text{for } 50 \leq Re_f \leq 1483 \\ &= 0.0504Re_f^{0.875} \quad \text{for } Re_f > 1483 \end{aligned} \quad (13)$$

$$Re_f = \frac{4\delta u_L \rho_L}{\eta_L} \quad (14)$$

where  $u_L$  is the average liquid velocity in the respective region.

For the forced convective coefficient at slug region, we used the Dittus–Boelter equation:

$$\alpha_{fc,s} = 0.023 \frac{\lambda_L}{D} Re_L^{0.8} Pr_L^{0.4} \quad (15)$$

where

$$Re_L = \frac{DU\rho_L}{\eta_L} \quad (16)$$

$$Pr_L = C_{pL}\eta_L/\lambda_L \quad (17)$$

where  $\eta_L$ ,  $\lambda_L$  and  $C_{pL}$  are the viscosity, thermal conductivity and the specific heat capacity of the liquid.

The nominal heat transfer coefficient for the slug region is then calculated from the expression

$$\alpha_s = \alpha_{fc,s} + \alpha_{nb,s} \quad (18)$$

where  $\alpha_{fc,s}$  and  $\alpha_{nb,s}$  are the forced convective and nucleate boiling coefficient calculated by the above methodology for the slug region.

Similarly for the film region we have:

$$\alpha_f = \alpha_{fc,f} + \alpha_{nb,f} \quad (19)$$

where  $\alpha_f$  is calculated for both the top and the bottom.

The average heat transfer coefficient for slug flow is given in Eq. (20):

$$\alpha = \alpha_s \frac{l_s}{l_u} + \alpha_f \frac{l_f}{l_u} \quad (20)$$

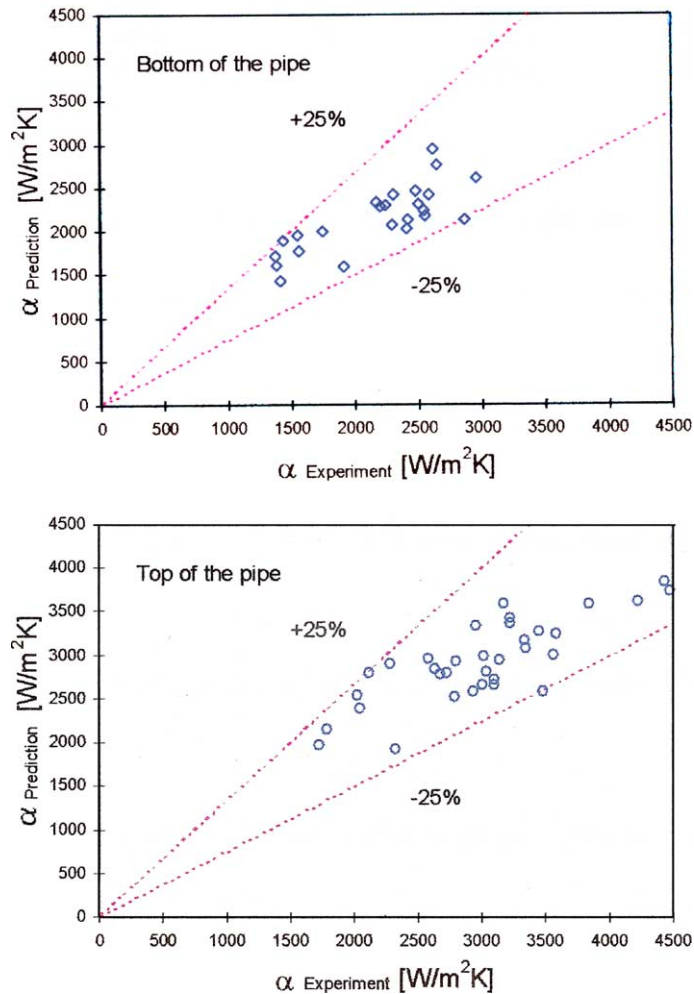


Fig. 8. The comparison between Eq. (20) and the data of Jung [1].

Fig. 8 shows a comparison between Jung's experimental data and predicted heat transfer coefficients. Most of the data are correlated within a deviation of  $\pm 25\%$ .

Bearing in mind the complexity of the analysis, this agreement is very satisfactory. More interesting than this overall agreement, however, is the distribution of the contribution to the average coefficient. This is illustrated in the block diagram shown in Fig. 9 where the contribution to the overall average heat transfer coefficient from nucleate boiling and forced convection, and from the slug region and the film region, respectively are shown for two different qualities. From this diagram, we conclude that

(1) The contribution to the overall coefficient of the slug region is small, most of the heat transfer occurring in the film region.

- (2) The forced convective coefficient in the lower film is greater than that at the top. Although the bottom film is thicker, it is more turbulent and moves with a higher velocity, giving a higher coefficient.
- (3) The nucleate boiling coefficient in the top film is more than that in the bottom. This is because the faster moving, more turbulent, bottom film gives rise to greater suppression in that region.
- (4) The contribution of the liquid slug region is about the same at the two qualities. At higher qualities, there are less liquid slugs but they travel quicker and have a higher convective heat transfer coefficient.

The slug flow region model presented here predicts a monotonic increase in the bottom coefficient with increasing quality and a monotonic decrease in the top coefficient. This is consistent with the data except at the



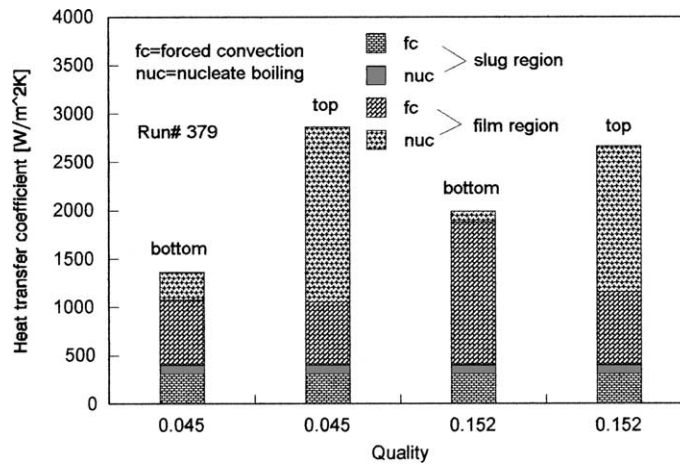


Fig. 9. The contribution to the overall average heat transfer coefficient from nucleate boiling and forced convection at the slug region and the film region.

lowest qualities (see Fig. 1) where the top coefficient increases slightly with quality and the bottom coefficient is fairly constant. Nevertheless, the general trends are captured.

## 6. Conclusions

The following main conclusions were drawn from this work:

- (1) The change of behaviour observed by Jung [1] in the evaporation of refrigerant-12 in the pipe appears to be well connected to the transition between slug flow and annular flow at a given quality.
- (2) There are strong differences between the cases of non-evaporative and evaporative heat transfer in tubes. In the former case, the heat transfer coefficient at the top of the tube is lower than at the bottom, with the reverse being true in the case of evaporation.
- (3) Application of the Coney [9] method to the prediction of the Jung [1] data indicated that the liquid film at the top of the tube was unlikely to dry out during the film drainage period following the passage of a liquid slug.
- (4) An analysis of the liquid behaviour in the film region has led the prediction of the mean heat transfer in the slug region with an accuracy of around  $\pm 25\%$ .
- (5) The analysis shows that heat transfer at the top of the tube could be dominated by nucleate boiling whereas that at the bottom is dominated by forced convection. Though the film at the top of the tube is very thin, it is also very slow moving compared

with the liquid layer at the bottom. Thus, suppression of nucleate boiling appears (from the present analysis) to be much greater in the bottom layer. This surprising conclusion needs to be further investigated.

## References

- [1] D.S. Jung, Horizontal-flow boiling heat transfer using refrigerant mixtures, EPRI Rep., 1989, ER-6364.
- [2] O. Shoham, A.E. Dukler, Y. Taitel, Heat transfer during intermittent/slug flow in horizontal tubes, *Ind. Eng. Fundam.* 2 (1982) 312–319.
- [3] T. Kago, T. Saruwatar, M. Kashima, S. Morooka, Y. Kato, Heat transfer in horizontal plug and slug flow for gas-liquid and gas-slurry systems, *J. Chem. Eng. Jpn.* 19 (2) (1986) 125–131.
- [4] S.D. Deshpande, A.A. Bishop, B.M. Karandikar, Heat transfer to air-water plug-slug flow in horizontal pipes, *Ind. Eng. Chem. Res.* 30 (1991) 2172–2180.
- [5] Y. Taitel, A.E. Dukler, A model for predicting flow regime transitions in horizontal and near horizontal gas-liquid flow, *AIChE* 22 (1976) 47–55.
- [6] A.E. Dukler, M.G. Hubbard, A model for gas-liquid slug flow in horizontal and near horizontal tubes, *Ind. Eng. Chem. Fundam.* 14 (1975) 337–347.
- [7] N.I. Heywood, J.F. Richardson, Slug flow of air-water mixtures in a horizontal pipe: Determination of liquid hold-up by  $\gamma$ -ray absorption, *Chem. Eng. Sci.* 34 (1979) 17–30.
- [8] G.A. Gregory, D.S. Scott, Correlation of liquid slug velocity and frequency in horizontal cocurrent gas-liquid slug flow, *AIChE* 15 (1969) 933–935.
- [9] M.W.E. Coney, The analysis of a mechanism of liquid replenishment and draining in horizontal two-phase flow, *Int. J. Multiphase Flow* 1 (1974) 647–669.

- [10] M.G. Cooper, Saturation nucleate pool boiling. A simple correlation, in: Proc. 1st UK National Conf. on Heat Transfer, vol. 2, 1984, pp. 785–793.
- [11] G.F. Hewitt, N.S. Hall-Taylor, *Annular Two-phase Flow*, Pergamon Press, Oxford, 1970.
- [12] K.E. Gungor, R.H.S. Winterton, A general correlation for flow boiling in tubes and annuli, *Int. J. Heat Mass Transfer* 29 (1986) 351–358.
- [13] G.F. Hewitt, G.L. Shires, T.R. Bott, *Process Heat Transfer*, CRC Press, Boca Raton, 1993.
- [14] J. Reimann, Experiments on the transition from slug to annular flow in horizontal air–water and steam–water flow, The Netherlands, 1981, 2–5 June, paper A8, p. 30.
- [15] J. Weisman, D. Duncan, J. Gibson, T. Crawford, Effects of liquid properties and pipe diameter on two-phase flow patterns in horizontal tubes, *Int. J. Multiphase Flow* 5 (1979) 437–462.
- [16] Sun, Guang, Heat transfer in convective flow boiling, Ph.D. thesis, London University, March, 1996.